Electronic Supplementary Material (ESI) for Inorganic Chemistry Frontiers.

Electronic Supplementary Information

Coordination framework materials fabricated by the self-assembly of Sn(IV) porphyrins with Ag(I) ions for the photocatalytic degradation of organic dyes in wastewater

Nirmal Kumar Shee, Hwa Jin Jo and Hee-Joon Kim*

Department of Applied Chemistry, Kumoh National Institute of Technology

61 Daehak-ro, Gumi 39177, Republic of Korea

List of contents:

Table S1. Crystallographic data and structure refinements for **1** and **2**.

	1	**2**
Empirical formula	$C_{40}H_{24}Ag_2N_8O_2Sn$	$C_{58}H_{38}Ag_2F_6N_{12}O_{10}S_2Sn$
Formula weight	983.1	1575.55
Crystal size (mm^3)	0.20 × 0.15 × 0.15	0.2 × 0.3 × 0.5
T (K)	173 (2)	223(2)
Crystal system, Space group	Orthorhombic, *Pmna*	Monoclinic, *C*2/*c*
Cell dimensions		
a (Å)	19.8288 (15)	17.616(3)
b (Å)	17.6770 (14)	24.301 (4)
c (Å)	8.5182 (7)	19.874 (4)
α (deg)	90.00	90.00
β (deg)	90.00	108.578 (3)
γ (deg)	90.00	90.00
V ($Å^3$)	2985.7 (4)	8064 (3)
Z, D_c (g cm^{-3})	2, 1.088	4, 1.298
μ (mm^{-1})	1.11	0.91
F(000)	1096	3120
θ range (°)	1.15 to 28.29	2.05 to 28.29
reflections collected	17461	23423
independent reflections (R_{int})	3710 (0.0635)	9377 (0.041)
absorption correction	None	None
data / restraints / parameters	3710 / 0 / 123	9377 / 3 / 410
GOF on F^2	0.9239	1.2774
$R1$,[a] $wR2$[b] [$I>2\sigma(I)$]	0.066, 0.1892	0.091, 0.2826
$R1$,[a] $wR2$[b] (all data)	0.1233, 0.2111	0.1261, 0.3422
Largest peak/hole (e $Å^{-3}$)	1.4586/ -1.6532	8.1412/-7.7329

[a] $R1 = \Sigma \| |F_o| - |F_c| \| / \Sigma |F_o|$. [b] $wR2 = [\Sigma[w(F_o^2 - F_c^2)^2] / \Sigma[w(F_o^2)^2]]^{1/2}$.

Table S2. Selected bond lengths [Å] and angles [°] for **1**.

Sn1-O1	2.069(7)	Sn1-N1	2.074(4)
Ag2-N2	2.052(14)	Ag3-N3	2.166(6)
O1-Sn1-O1	180.0(4)	O1-Sn1-N1	88.7(2)
O1-Sn1-N1	91.3(2)	O1-Sn1-N1	88.7(2)
O1-Sn1-N1	91.3(2)	N1-Sn1-N1	90.3(2)
O1-Sn1-N1	91.3(2)	O1-Sn1-N1	88.7(2)
N1-Sn1-N1	180.0(8)	N1-Sn1-N1	89.7(2)
O1-Sn1-N1	91.3(2)	O1-Sn1-N1	88.7(2)
N1-Sn1-N1	89.7(2)	N1-Sn1-N1	180.0(1)
N1-Sn1-N1	90.3(2)	N2-Ag2-N2	180.0(10)
N3-Ag3-N3	180.0(5)	C2-N1-Sn1	125.8(3)
C5-N1-Sn1	125.5(4)	C9-N3-Ag3	119.5(4)
C13-N2-Ag2	122(2)	C12-N2-Ag2	127.0(16)

Symmetry codes: (i) −*x*+1, −*y*+1, −*z*+1; (ii) −*x*+1, *y*, *z*; (iii) *x*, −*y*+1, −*z*+1; (iv) −*x*+1, −*y*+2, −*z*; (v) −*x*, −*y*+1, −*z*+1.

Table S3. Selected bond lengths [Å] and angles [°] for **2**.

Sn1-O1	2.066(5)	Sn1-N2	2.081(5)
Sn1-N1	2.087(5)	Ag1-N6	2.198(6)
Ag1-N4	2.373(9)	Ag2-N3	2.216(6)
Ag2-N5	2.443(9)		

O1-Sn1-O1	178.9(3)	O1-Sn1-N2	94.7(2)
O1-Sn1-N2	86.1(2)	O1-Sn1-N2	94.7(2)
N2-Sn1-N2	89.6(3)	O1-Sn1-N1	85.0(2)
O1-Sn1-N1	94.2(2)	N2-Sn1-N1	179.7(2)
N2-Sn1-N1	90.3(2)	O1-Sn1-N1	94.2(2)
O1-Sn1-N1	85.0(2)	N2-Sn1-N1	90.3(2)
N2-Sn1-N1	179.7(2)	N1-Sn1-N1	89.8(3)
N6-Ag1-N6	149.7(4)	N6-Ag1-N4	105.16(18)
N3-Ag2-N3	165.0(3)	N3-Ag2-N5	97.48(16)
C23-O1-Sn1	129.2(5)	C1-N1-Sn1	126.2(4)
C4-N1-Sn1	125.2(4)	C14-N2-Sn1	125.8(4)
C11-N2-Sn1	125.2(4)	C9-N3-Ag2	124.5(6)
C8-N3-Ag2	118.1(5)	C18-N4-Ag1	121.9(5)
C22-N5-Ag2	121.3(5)	C27-N6-Ag1	118.2(6)
C26-N6-Ag1	124.2(5)		

Symmetry codes: (i) −*x*+2, *y*, −*z*+3/2; (ii) −*x*+2, *y*, −*z*+1/2; (iii) −*x*+2, −*y*, −*z*+1; (iv) *x*+1/2, *y*+1/2, *z*; (v) *x*−1/2, *y*−1/2, *z*.

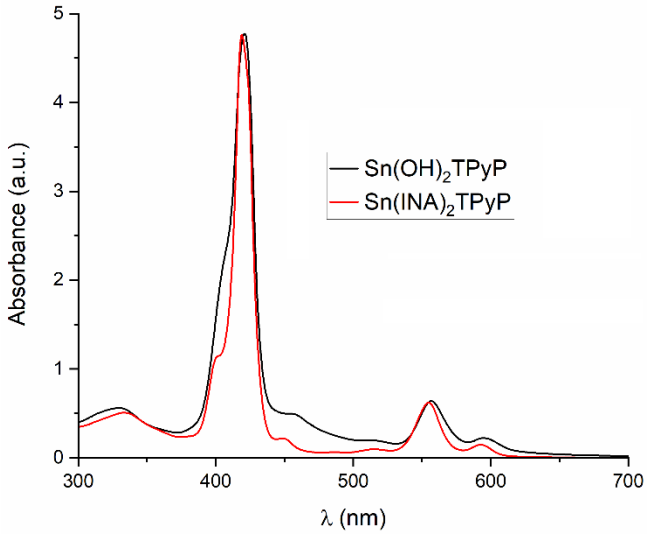

Fig. S1 UV-vis absorption spectra of $Sn(OH)_2TPyP$ and $Sn(INA)_2TPyP$ in chloroform.

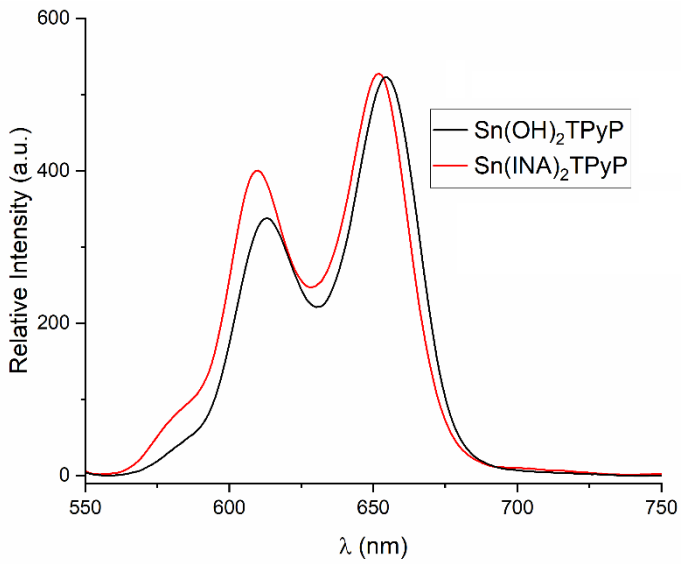

Fig. S2 Fluorescence spectra of $Sn(OH)_2TPyP$ and $Sn(INA)_2TPyP$ (excited at 560 nm) in chloroform.

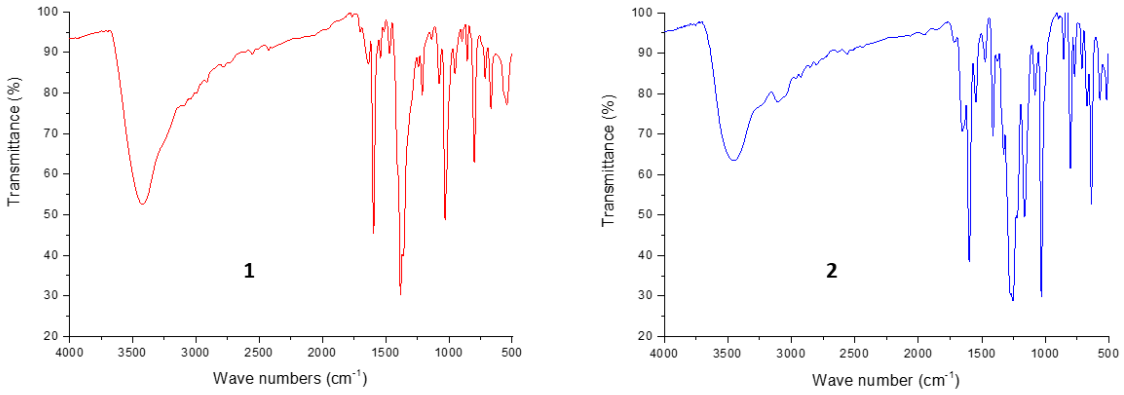

Fig. S3 FT-IR spectra of **1** and **2**.

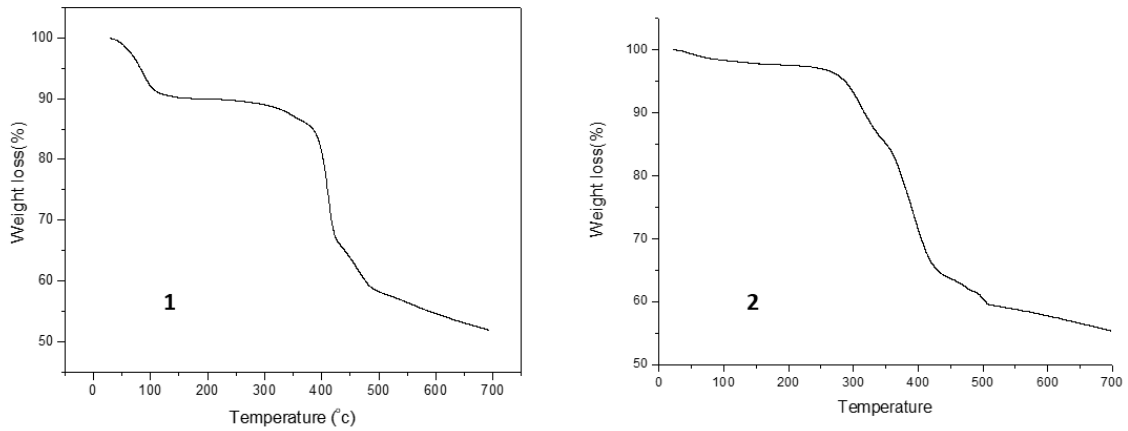

Fig. S4 TGA curves of **1** and **2**.

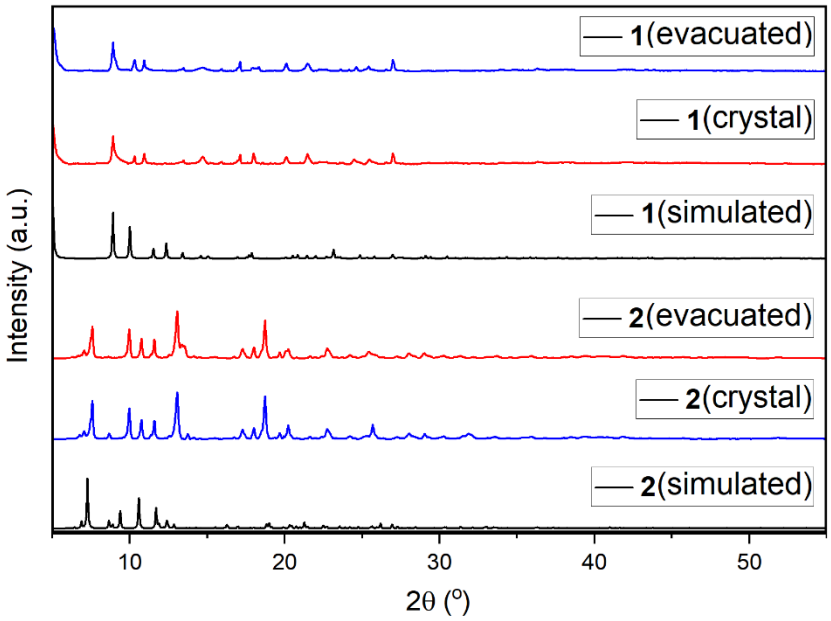

Fig. S5 Powder X-ray diffraction (PXRD) patterns of **1** and **2**.

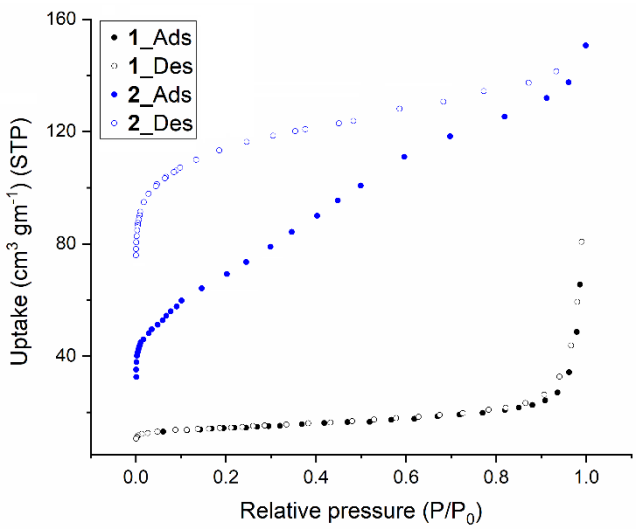

Fig. S6 Adsorption and desorption isotherms of N_2 for **1** and **2** at 77 K.

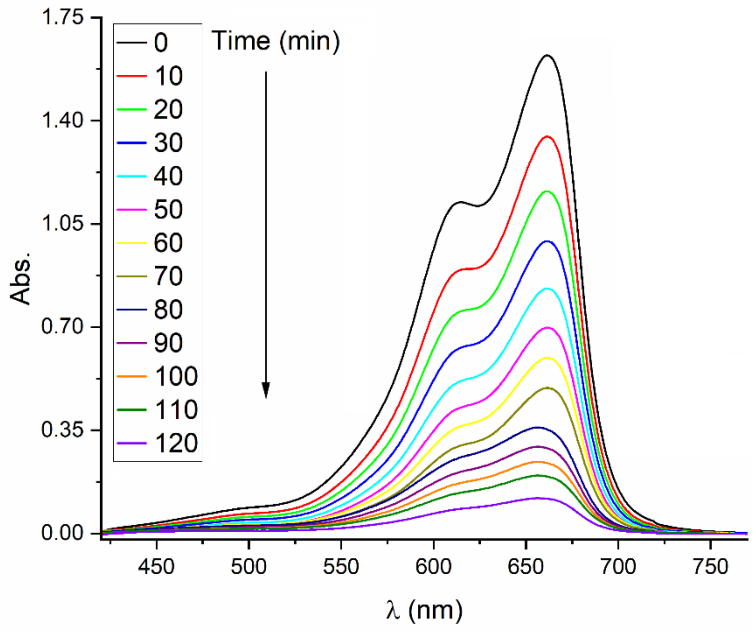

Fig. S7 Time-dependent absorption spectra of MB in the presence of **2** under visible light irradiation.

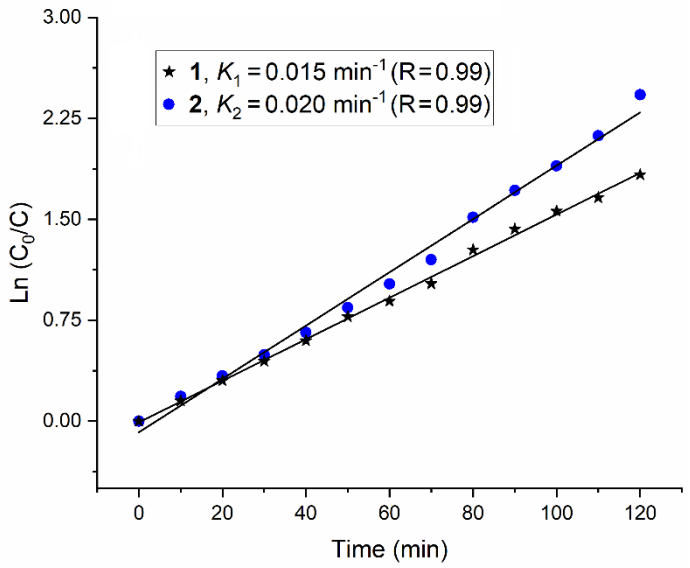

Fig. S8 Kinetics for the photocatalytic degradation of MB under visible light irradiation by photocatalysts **1** and **2**.

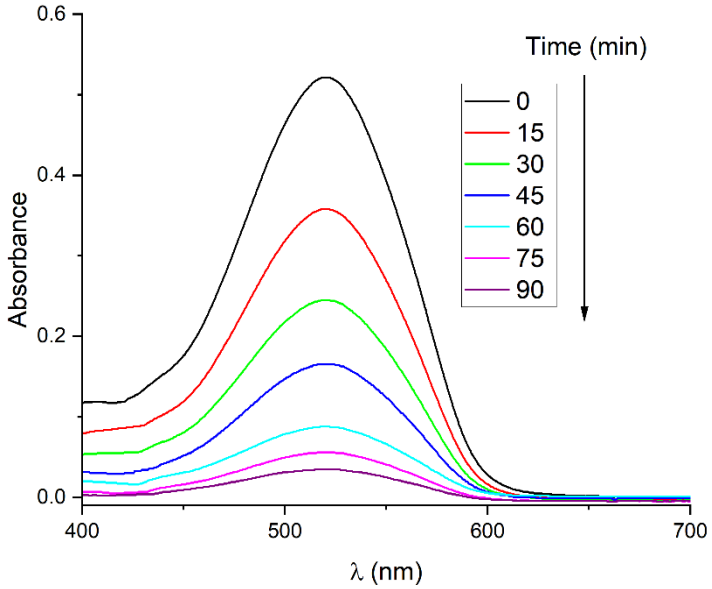

Fig. S9 Time-dependent absorption spectra of AM in the presence of **2** under visible light irradiation.

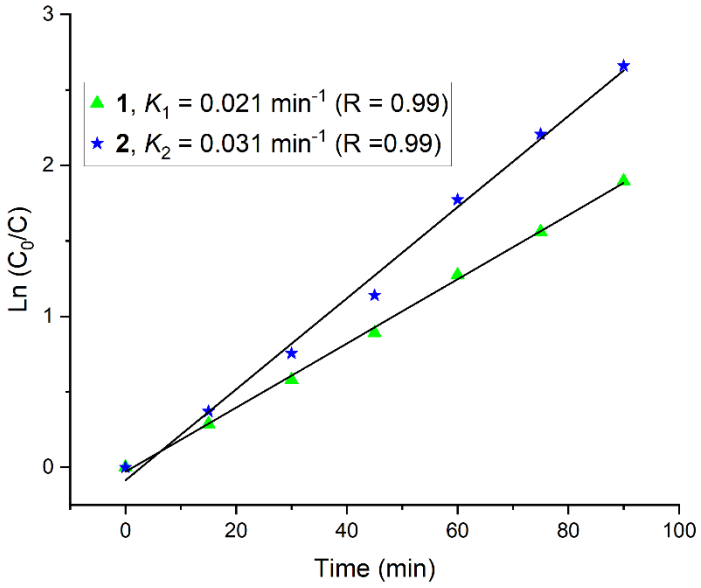

Fig. S10 Kinetics-for the photocatalytic degradation of AM under visible light irradiation by photocatalysts **1** and **2**.

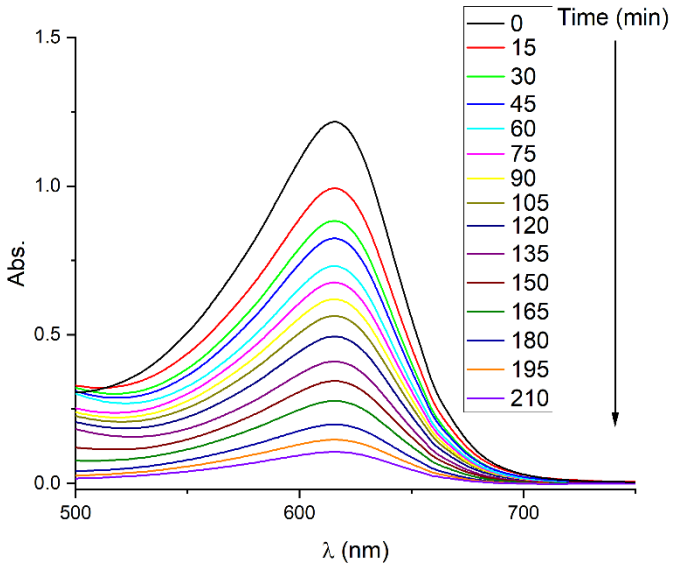

Fig. S11 Time-dependent absorption spectra of BCG in the presence of **2** under visible light irradiation.

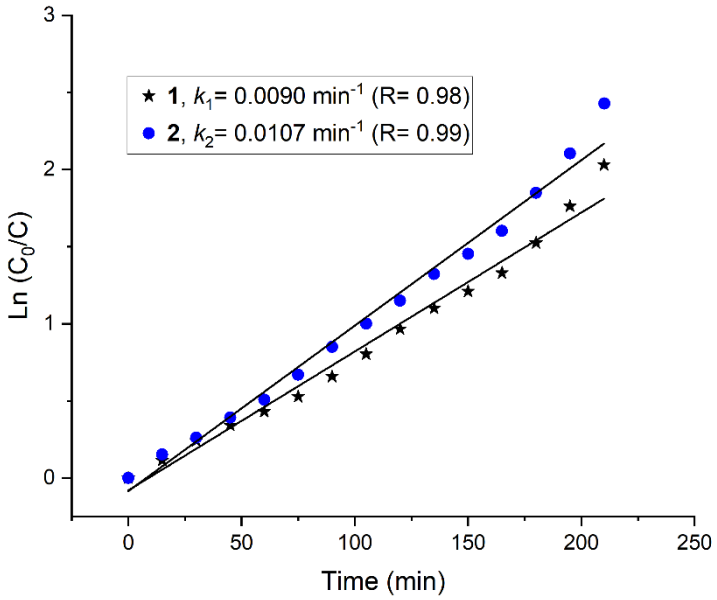

Fig. S12 Kinetics for the photocatalytic degradation of BCG under visible light irradiation by photocatalysts **1** and **2**.

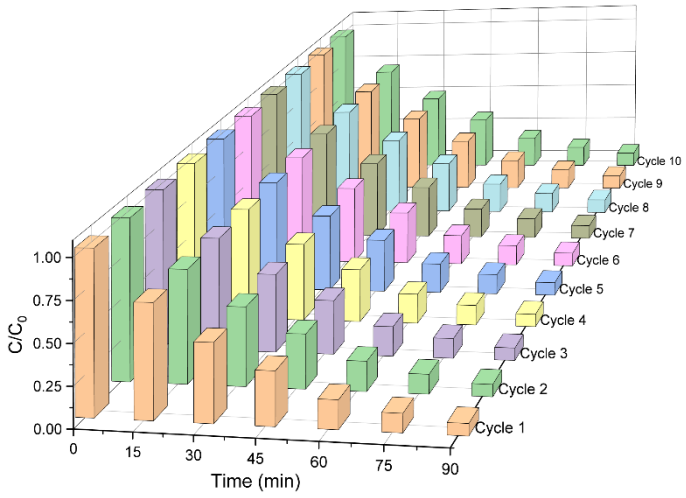

Fig. S13 Catalytic cycles (up to 10 cycles) for photo-catalyst **2** for the degradation of AM dye.

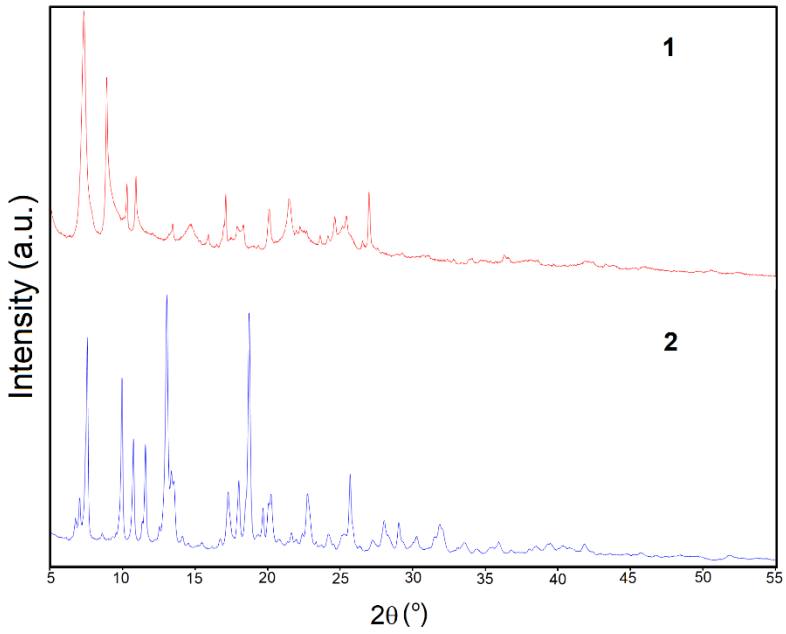

Fig. S14 Powder X-ray diffraction (PXRD) patterns of **1** and **2** after use for photocatalytic degradation of AM dye.

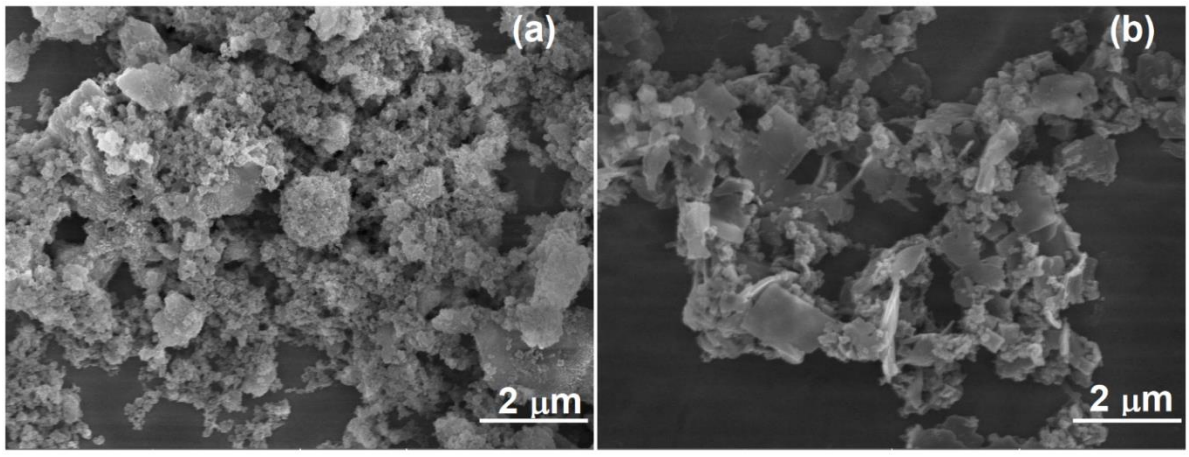

Fig. S15 FE-SEM images of photocatalyst **1** and **2** after the degradation of AM dye.

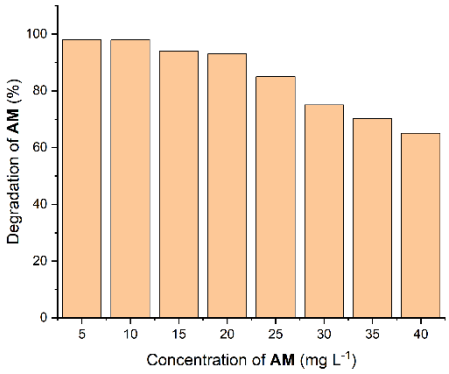

Fig. S16 Concentration effect of AM dye on the photo-degradation by **2** (5 mg) within 90 min of visible light irradiation.

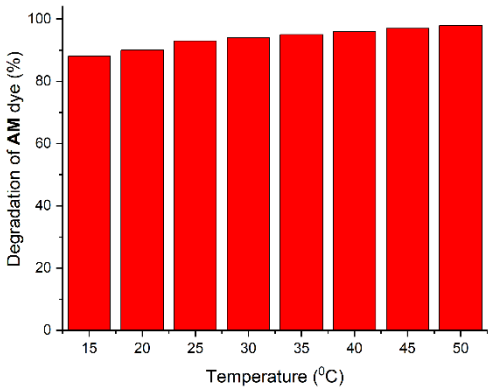

Fig. S17 Effect of temperature on the degradation of AM dye by **2**.

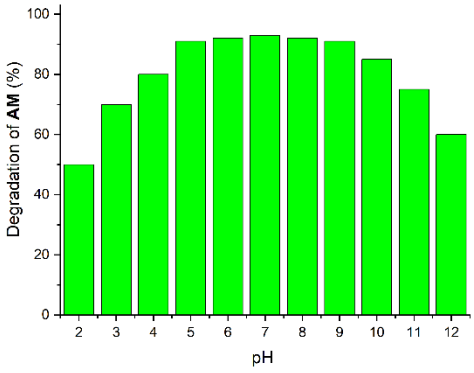

Fig. S18 pH Effect of AM dye solution on the photo-degradation of by **2**.

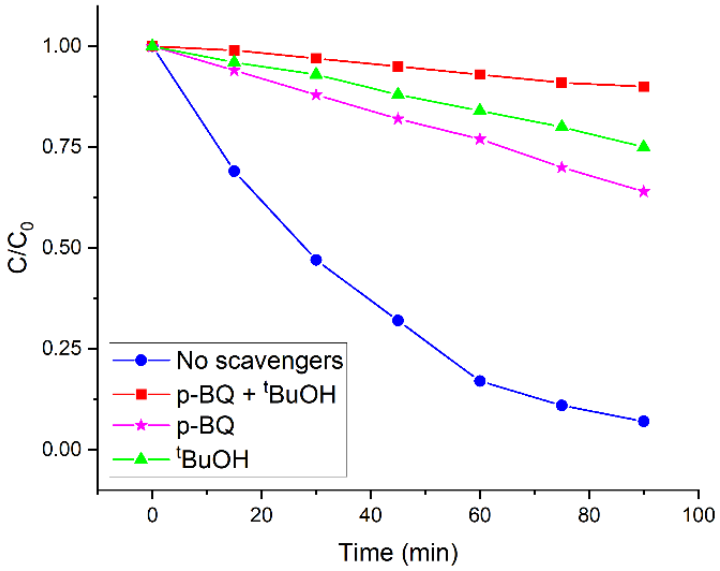

Fig. S19 Effect of various scavengers on the degradation of AM dye in the presence of **2** under visible light irradiation.

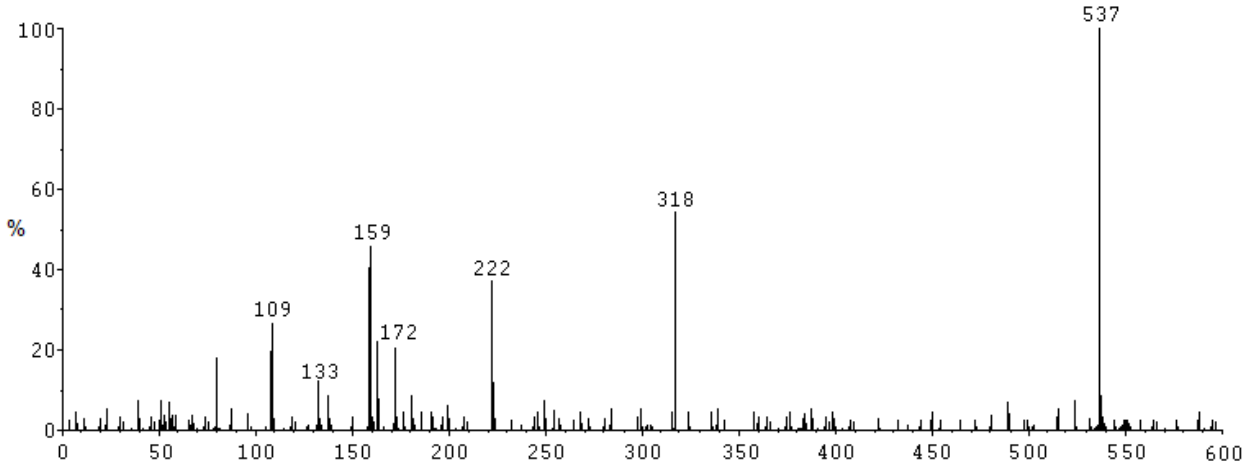

Fig. S20 ESI-MS spectrum (negative ion mode) of the reaction mixture of AM in the presence of **2** after 60 min of visible light irradiation.
